ICES REPORT 10-13

March 2010

Discontinuous Petrov-Galerkin Method with Optimal Test Functions for Thin-Body Problems in Solid Mechanics

by

Antti H. Niemi, Jamie A. Bramwell, and Leszek F. Demkowicz

The Institute for Computational Engineering and Sciences
The University of Texas at Austin
Austin, Texas 78712

Reference: Antti H. Niemi, Jamie A. Bramwell, and Leszek F. Demkowicz, "Discontinuous Petrov-Galerkin Method with Optimal Test Functions for Thin-Body Problems in Solid Mechanics", ICES REPORT 10-13, The Institute for Computational Engineering and Sciences, The University of Texas at Austin, March 2010.

Discontinuous Petrov-Galerkin Method with Optimal Test Functions for Thin-Body Problems in Solid Mechanics

Antti H. Niemi*, Jamie A. Bramwell†, Leszek F. Demkowicz‡

Institute for Computational Engineering and Sciences
The University of Texas at Austin
1 University Station C0200
Austin, Texas 78712

Abstract

We study the applicability of the discontinuous Petrov-Galerkin (DPG) variational framework for thin-body problems in structural mechanics. Our numerical approach is based on discontinuous piecewise polynomial finite element spaces for the trial functions and approximate, local computation of the corresponding 'optimal' test functions. In the Timoshenko beam problem, the proposed method is shown to provide the best approximation in an energy-type norm which is equivalent to the L_2-norm for all the unknowns, uniformly with respect to the thickness parameter. The same formulation remains valid also for the asymptotic Euler-Bernoulli solution. As another one-dimensional model problem we consider the modelling of the so called basic edge effect in shell deformations. In particular, we derive a special norm for the test space which leads to a robust method in terms of the shell thickness. Finally, we demonstrate how a posteriori error estimator arising directly from the discontinuous variational framework can be utilized to generate an optimal *hp*-mesh for resolving the boundary layer.

Acknowledgements This work was made possible with funding from King Abdullah University of Science and Technology (KAUST). We are grateful for this financial support.

*ahniemi@ices.utexas.edu
†jamie.bramwell@gmail.com
‡leszek@ices.utexas.edu

1 Introduction

In this paper, a finite element framework proposed recently in [1, 2] is adapted for solving thin-body problems in solid mechanics. The method under study is of Petrov-Galerkin type and has its roots in the early methodology developed by Barrett and Morton [3] to symmetrize non-symmetric problems using the concept of optimal test functions. In fact, a similar approach with so called numerically optimal test functions was taken in [4, 5]. However, it was not until very recently when it was discovered that certain variational formulations of discontinuous Petrov-Galerkin (DPG) type allow a practical computation of an optimal test space for stability. More precisely, it was shown in [2] that if fully discontinuous finite element spaces are used for both trial and test functions, as in the DPG method of Bottasso et al. [6], the optimal test functions can be approximated locally in an enriched finite element space. In addition, a similar procedure can also be used to compute local a posteriori error estimates to guide adaptive mesh refinements as demonstrated in [7] in the context of convection-dominated diffusion problems.

The goal of the present study is to find out how the good performance of the DPG method with optimal test functions demonstrated previously in flow problems carries over to problems in solid mechanics involving thin structures, such as beams, plates, and shells. Common to these problems is the presence of a small thickness parameter whose value can have a radical effect on the quality of finite element solutions. Nowadays, such parametric error amplification effects, or locking effects, and their numerical remedies are rather well understood for the one-dimensional beam and arch problems whereas some questions remain open for the two-dimensional plate and shell problems, see e.g [8] and the references therein. Part of the open problems are related to the presence of strong boundary layers which are common in shell deformations [9, 10, 11, 12], but possible also in the Reissner-Mindlin plate model near free or simply supported edges [13, 14].

It should be noted that Petrov-Galerkin finite element formulations for elasticity have been proposed and studied earlier in the series of articles by Loula, Hughes, Franca and Miranda, see [15, 16, 17, 18]. Their starting point has been either the classical principle of virtual work (displacement formulation) or the variational principle of Hellinger and Reissner (displacement-stress formulation). We deviate from these conventional continuum mechanics approaches by deriving a variational formulation directly for the first-order system of differential equations corresponding to the constitutive laws and the fundamental balance laws of momentum and angular momentum. Part of the motivation for this comes from the possibility to extend the formulation to generalized Cosserat, or micropolar continuum.

The paper is structured as follows. We start our discussion in Section 2 by deriving a discontinuous Petrov-Galerkin variational formulation for the Timoshenko beam problem. We continue the study by presenting a stability analysis for the optimal DPG method followed by some numerical computations confirming the theoretical results. Section 3 focuses then on the one-dimensional problem related to the basic edge effect in shell deformations. We analyze a simplified model problem for the boundary layer which actually resembles closely the beam problem. We demonstrate numerically how the robustness of the method depends on the choice of the norm for the test functions. Finally, the paper is closed with some

concluding remarks in Section 4.

We use standard notation where $L_2(0,1)$ stands for the set of square integrable functions defined on the interval $(0,1)$ equipped with the norm

$$\|v\| = \left\{ \int_0^1 v^2 \, \mathrm{d}x \right\}^{1/2}$$

and $H^1(0,1)$ denotes the standard Sobolev space

$$H^1(0,1) = \{v \ \mid \ v \in L_2(0,1), \ v' \in L_2(0,1)\}$$

2 The Timoshenko beam model

According to the Timoshenko beam model, the kinematics of the beam are characterized by the transverse deflection w and and the rotation ψ of the beam's cross section

$$w = w(x), \quad \psi = \psi(x), \quad 0 \le x \le L$$

where x denotes the axial coordinate and L is the length of the beam. In the model the shear force V and the bending moment M are specified by the constitutive equations

$$V = \gamma GA \left(\frac{dw}{dx} - \psi \right), \quad M = EI \frac{d\psi}{dx} \tag{1}$$

where E and G are the Young and shear modulus of the material. The symbol I stands for the moment of inertia about the beam axis whereas A denotes the area of the beam's cross section. Moreover, the shear correction factor γ can be introduced to modify the shear modulus to take into account variations of the shear strain over the beam's cross section. The balance equations of static equilibrium can then be written in the form

$$-\frac{dV}{dx} = p, \quad -\frac{dM}{dx} - V = m \tag{2}$$

where the loading functions $p = p(x)$ and $m = m(x)$ are the distributed force and moment, respectively. Above we have adopted the sign convention used in [15].

Upon rescaling the coordinate and the kinematic quantities as

$$x \hookrightarrow Lx, \quad w \hookrightarrow Lw, \quad \psi \hookrightarrow \psi$$

and the stress quantities as

$$V \hookrightarrow GAV, \quad M \hookrightarrow EIL^{-1}M, \quad p \hookrightarrow GALp, \quad m \hookrightarrow EIL^2 m$$

we arrive from (2) and (1) at the dimensionless system of equations

$$\begin{aligned} V &= \gamma(w' - \psi), \quad & M &= \psi' \\ -V' &= p, & -M' - kV &= m \end{aligned} \tag{3}$$

where $k = GAL^2/EI$.

Model problem: cantilever with tip load

Let us assume that the cross section of the beam is a rectangle of width b and thickenss d so that $A = bd$, $I = bd^3/12$ and $k = 12G/Et^{-2}$, where $t = d/L$ denotes the dimensionless thickness of the beam. When the beam is thin, i.e. $t \ll 1$, the moment M becomes the dominant reaction and it is convenient to normalize its amplitude to that of the loading by rescaling V and p as

$$V \hookrightarrow t^2 V, \quad p \hookrightarrow t^2 p$$

The beam equations (3) take then the form

$$\begin{aligned} t^2 V &= \gamma(w' - \psi), & M &= \psi' \\ -V' &= p, & -M' - kV &= m \end{aligned} \tag{4}$$

where k has been redefined as $k = 12G/E$.

In our model probem, the distributed loads are set to zero, $p(x) \equiv 0$, $m(x) \equiv 0$ and the beam is loaded at $x = 1$ by a normal force of the (scaled) magnitude F while restraining the other end at $x = 0$ completely from moving. This leads to natural boundary conditions

$$V(1) = F, \quad M(1) = 0$$

and kinematic constraints

$$w(0) = 0, \quad \psi(0) = 0$$

The problem above can be solved by integration and the solution (Green's function for transversal loads) is

$$\begin{aligned} V &= F, & M &= -kF(x-1) \\ \psi &= kF\left(x - \frac{1}{2}x^2\right), & w &= \frac{kF}{2}\left(x^2 - \frac{x^3}{3}\right) + \frac{Ft^2}{\gamma}x \end{aligned}$$

Variational formulation

In this section, we follow [2] and derive a Petrov-Galerkin method with optimal test functions for the beam problem. We start by considering a weak, one-element formulation of the nondimensional form (4) of the problem, which reads as follows: Find the internal and boundary fields $\mathbf{u} = (V, M, \psi, w) \times (\hat{V}(0), \hat{M}(0), \hat{\psi}(1), \hat{w}(1)) \in \mathcal{U}$ such that

$$\begin{aligned} t^2 \int_0^1 Vq\,\mathrm{d}x \qquad & +\gamma \int_0^1 wq'\,\mathrm{d}x - \gamma\hat{w}(1)q(1) + \gamma \int_0^1 \psi q\,\mathrm{d}x && = 0 \\ \int_0^1 M\tau\,\mathrm{d}x \qquad & + \int_0^1 \psi\tau'\,\mathrm{d}x - \hat{\psi}(1)\tau(1) && = 0 \\ \int_0^1 Vz'\,\mathrm{d}x + \hat{V}(0)z(0) & && = Fz(1) \\ k\int_0^1 V\phi\,\mathrm{d}x - \int_0^1 M\phi'\,\mathrm{d}x \quad & - \hat{M}(0)\phi(0) && = 0 \end{aligned} \tag{5}$$

for all test functions $\mathbf{v} = (q, \tau, z, \phi) \in \mathcal{V}$. The variational problem is meaningful if we set $\mathcal{U} = [L_2(0,1)]^4 \times \mathbb{R}^4$, $\mathcal{V} = [H^1(0,1)]^4$ and may be written in the abstract form

$$\mathbf{u} \in \mathcal{U}: \quad \mathcal{B}(\mathbf{u}, \mathbf{v}) = \mathcal{L}(\mathbf{v}) \quad \forall \mathbf{v} \in \mathcal{V} \tag{6}$$

where $\mathcal{B}(\cdot,\cdot)$ is the bilinear form defined as the sum of the left-hand sides in (5) and $\mathcal{L}(\mathbf{v}) = Fz(1)$.

In order to show that the above problem is well posed, the Hilbert space $\mathcal{U}$ is a equipped with a generalized energy norm defined as the dual norm

$$|\!|\!| \mathbf{u} |\!|\!| \doteq \sup_{\mathbf{v} \in \mathcal{V}} \frac{\mathcal{B}(\mathbf{u}, \mathbf{v})}{\|\mathbf{v}\|_{\mathcal{V}}} \tag{7}$$

Notice that the characteristics of the energy norm depend on the choice of the norm $\|\cdot\|_{\mathcal{V}}$. In particular, if the regular Hilbert space norm

$$\|\mathbf{v}\|_{\mathcal{V}}^2 = \|q\|_V^2 + \|\tau\|_V^2 + \|z\|_V^2 + \|\psi\|_V^2\,, \qquad \|v\|_V^2 = \|v'\|^2 + \|v\|^2 \tag{8}$$

corresponding to an inner product $(\cdot,\cdot)_{\mathcal{V}}$ is used, the energy norm of a given $\mathbf{u}$ is characterized as $|\!|\!| \mathbf{u} |\!|\!| = \|\mathbf{T}\mathbf{u}\|_{\mathcal{V}}$ where $\mathbf{T}\mathbf{u}$ is the Riesz representation of $\mathcal{B}(\mathbf{u}, \cdot) \in \mathcal{V}'$ in $\mathcal{V}$:

$$(\mathbf{T}\mathbf{u}, \delta\mathbf{v})_{\mathcal{V}} = \mathcal{B}(\mathbf{u}, \delta\mathbf{v}) \quad \forall \delta\mathbf{v} \in \mathcal{V} \tag{9}$$

The following result relates the new energy norm to more standard norms in $\mathcal{U}$ such as

$$\|\mathbf{u}\|_{\mathcal{U}} = \max\left\{ \|V\|, \|M\|, \|w\|, \|\theta\|, |\hat{V}(0)|, |\hat{M}(0)|, |\hat{w}(1)|, |\hat{\theta}(1)| \right\} \tag{10}$$

Theorem 2.1. *Let $\mathbf{u} \in \mathcal{U} = [L_2(0,1)]^4 \times \mathbb{R}^4$. Then there exists two positive constants C_1 and C_2 both independent of the thickness parameter t such that*

$$C_1 \|\mathbf{u}\|_{\mathcal{U}} \le |\!|\!| \mathbf{u} |\!|\!| \le C_2 \|\mathbf{u}\|_{\mathcal{U}} \tag{11}$$

where $|\!|\!| \cdot |\!|\!|$ is the energy norm defined by (7), (8) *and $\|\cdot\|_{\mathcal{U}}$ is the norm* (10).

Proof. Our proof is based on construction of an explicit expression for the energy norm. This can be accomplished by working, instead of (8), with an equivalent test space norm

$$\|v\|_V^2 = \|v'\|^2 + |v(1)|^2 \tag{12}$$

Testing individually with the components of $\delta\mathbf{v} = (\delta q, \delta\tau, \delta z, \delta\phi)$ in (9) together with (12) leads us to four variational problems for the components of $\mathbf{v}_{\mathbf{u}} = (q, \tau, z, \phi)$:

$$\begin{aligned}
\int_0^1 q'\delta q'\,\mathrm{d}x + q(1)\delta q(1) =& t^2 \int_0^1 V\delta q\,\mathrm{d}x + \gamma \int_0^1 w\delta q'\,\mathrm{d}x - \hat{w}(1)\delta q(1) \\
&+ \gamma \int_0^1 \psi\delta q\,\mathrm{d}x \quad \forall \delta q \in H^1(0,1) \\
\int_0^1 \tau'\delta\tau'\,\mathrm{d}x + \tau(1)\delta\tau(1) =& \int_0^1 M\delta\tau\,\mathrm{d}x + \int_0^1 \psi\delta\tau'\,\mathrm{d}x - \hat{\psi}(1)\delta\tau(1) \quad \forall \delta\tau \in H^1(0,1) \\
\int_0^1 z'\delta z'\,\mathrm{d}x + z(1)\delta z(1) =& \int_0^1 V\delta z'\,\mathrm{d}x + \hat{V}(0)\delta z(0) \quad \forall \delta z \in H^1(0,1) \\
\int_0^1 \phi'\delta\phi'\,\mathrm{d}x + \phi(1)\delta\phi(1) =& k\int_0^1 V\delta\phi\,\mathrm{d}x - \int_0^1 M\delta\phi'\,\mathrm{d}x + \hat{M}(0)\delta\phi(0) \quad \forall \delta\phi \in H^1(0,1)
\end{aligned}$$

The corresponding classical boundary value problems obtained by integration by parts are

$$\begin{cases} -q'' = t^2 V - \gamma(w' - \psi) \\ q'(0) = \gamma w(0) \\ q'(1) + q(1) = \gamma(w(1) - \hat{w}(1)) \end{cases} \qquad \begin{cases} -\tau'' = M - \psi' \\ \tau'(0) = \psi(0) \\ \tau'(1) + \tau(1) = \psi(1) - \hat{\psi}(1) \end{cases}$$

$$\begin{cases} -z'' = -V' \\ z'(0) = V(0) - \hat{V}(0) \\ z'(1) + z(1) = V(1) \end{cases} \qquad \begin{cases} -\phi'' = kV + M' \\ \phi'(0) = -M(0) - \hat{M}(0) \\ \phi'(1) + \phi(1) = -M(1) \end{cases}$$

These can be solved for

$$\begin{cases} -q' = t^2 \int_0^x V - \gamma\big(w - \int_0^x \psi\big) \\ q(1) = t^2 \int_0^1 V - \gamma\big(\hat{w}(1) - \int_0^1 \psi\big) \end{cases} \qquad \begin{cases} -\tau' = \int_0^x M - \psi \\ \tau(1) = \int_0^1 M - \hat{\psi}(1) \end{cases}$$

$$\begin{cases} -z' = -V + \hat{V}(0) \\ z(1) = \hat{V}(0) \end{cases} \qquad \begin{cases} -\phi' = k \int_0^x V + M + \hat{M}(0) \\ \phi(1) = k \int_0^1 V + \hat{M}(0) \end{cases} \tag{13}$$

where $\int_0^x$ and $\int_0^1$ denote the usual operations of indefinite and definite integration. The above expressions give rise to the energy norm

$$\begin{aligned} |\!|\!| \mathbf{u} |\!|\!|^2 = {} & \left\| -V + \hat{V}(0) \right\|^2 + \left| \hat{V}(0) \right|^2 + \left\| k \int_0^x V + M + \hat{M}(0) \right\|^2 + \left| k \int_0^1 V + \hat{M}(0) \right|^2 \\ & + \left\| t^2 \int_0^x V - \gamma\big(w - \int_0^x \psi\big) \right\|^2 + \left| t^2 \int_0^1 V - \gamma\big(\hat{w}(1) - \int_0^1 \psi\big) \right|^2 \\ & + \left\| \int_0^x M - \psi \right\|^2 + \left| \int_0^1 M - \hat{\psi}(1) \right|^2 \end{aligned}$$

Cauchy-Schwarz inequality implies that

$$\left\| \int_x^1 v \right\|, \ \left| \int_0^1 v \right| \leq \|v\| \tag{14}$$

for any $v \in L_2(0,1)$ so that the upper bound in (11) follows from the triangle inequality. The lower bound is rather straightforward as well because of the direct control of the term $|\hat{V}(0)|$ in the energy norm. □

Theorem 2.1 implies that the bilinear form $\mathcal{B}(\mathbf{u}, \mathbf{v})$ is continuous with the constant C_2 and satisfies the Babuška-Brezzi condition with the constant C_1. The existence and uniqueness for problem (6) follow from Banach's closed range theorem (see e.g. [19, Section 5.17]) since the subspace

$$\{\mathbf{v} \in \mathcal{V} \mid \mathcal{B}(\mathbf{u}, \mathbf{v}) = 0 \quad \forall \mathbf{u} \in \mathcal{U}\}$$

is trivial.

Discontinuous Petrov-Galerkin method with optimal test functions

Let $\mathcal{U}_n$ be a finite dimensional subspace of $\mathcal{U}$ corresponding to a linearly independent set of trial functions $\mathbf{e}_1, \ldots, \mathbf{e}_n \in \mathcal{U}$ as

$$\mathcal{U}_n = \text{span}\{\mathbf{e}_1, \ldots, \mathbf{e}_n\} \tag{15}$$

Upon defining the optimal test space as

$$\mathcal{V}_n^{\text{opt}} = \text{span}\{\mathbf{Te}_1, \ldots, \mathbf{Te}_n\} \tag{16}$$

we arrive at the following symmetrized Petrov-Galerkin method for the approximation of (6):

$$\mathbf{u}_n \in \mathcal{U}_n : \quad \mathcal{B}(\mathbf{u}_n, \mathbf{v}_n) = \mathcal{L}(\mathbf{v}_n) \quad \forall \mathbf{v}_n \in \mathcal{V}_n^{\text{opt}} \tag{17}$$

This formulation is symmetric because each $\mathbf{v}_n \in \mathcal{V}_n^{\text{opt}}$ may be written as $\mathbf{v}_n = \mathbf{Tw}_n$ for some $\mathbf{w}_n \in \mathcal{U}_n$ so that (17) can be expressed as

$$(\mathbf{Tu}_n, \mathbf{Tw}_n)_{\mathcal{V}} = \mathcal{L}(\mathbf{Tw}_n) \quad \forall \mathbf{w}_n \in \mathcal{U}_n$$

Because the exact solution $\mathbf{u}$ satisfies the same formulation, the subspace solution $\mathbf{u}_n$ is the best approximation of $\mathbf{u}$ in the generalized energy norm,

$$|\!|\!| \mathbf{u} - \mathbf{u}_n |\!|\!| = \min_{\mathbf{w}_n \in \mathcal{U}_n} |\!|\!| \mathbf{u} - \mathbf{w}_n |\!|\!|$$

and, according to Theorem 2.1, the best approximation of $\mathbf{u}$ up to the constant C_2/C_1 in the standard norm

$$\|\mathbf{u} - \mathbf{u}_n\|_{\mathcal{U}} \leq \frac{C_2}{C_1} \min_{\mathbf{w}_n \in \mathcal{U}_n} \|\mathbf{u} - \mathbf{w}_n\|_{\mathcal{U}} \tag{18}$$

If the trial space $\mathcal{U}_n$ of Eq. (15) is a typical finite element space consisting of piecewise polynomial functions associated to an arbitrary partition

$$\mathcal{T}_h : \quad 0 = x_0 < x_1 < x_2 < \cdots < x_N = 1 \tag{19}$$

the symmetrization of the variational problem can be carried out in a practical manner as follows [2, 7]. In addition to $\mathbf{u}_n = (V, M, w, \psi) \times (\hat{V}(0), \hat{M}(0), \hat{w}(1), \hat{\psi}(1)) \in \mathcal{U}_n$, we treat as independent unknowns the interface variables $\boldsymbol{\lambda}_h = (\hat{\mathbf{V}}, \hat{\mathbf{M}}, \hat{\mathbf{w}}, \hat{\boldsymbol{\psi}}) \in \boldsymbol{\Lambda}_h = \mathbb{R}^{4N-4}$ corresponding to the internal nodes $x_1, \ldots, x_{N-1}$:

$$\hat{\mathbf{V}} = (\hat{V}(x_1), \ldots, \hat{V}(x_{N-1})) \qquad \hat{\mathbf{M}} = (\hat{M}(x_1), \ldots, \hat{M}(x_{N-1}))$$
$$\hat{\mathbf{w}} = (\hat{w}(x_1), \ldots, \hat{w}(x_{N-1})) \qquad \hat{\boldsymbol{\psi}} = (\hat{\psi}(x_1), \ldots, \hat{\psi}(x_{N-1}))$$

We define then the bilinear form

$$\begin{aligned}\mathcal{B}_h(\mathbf{u}_n,\boldsymbol{\lambda}_h;\mathbf{v}) = \sum_{j=1}^{N}\Bigg\{ & t^2\int_{x_{j-1}}^{x_j} Vq_j\,\mathrm{d}x + \gamma\int_{x_{j-1}}^{x_j} wq_j'\,\mathrm{d}x - \gamma\hat{w}(x)q_j(x)\Big|_{x_{j-1}}^{x_j} + \gamma\int_{x_{j-1}}^{x_j}\psi q_j\,\mathrm{d}x \\ & + \int_{x_{j-1}}^{x_j} M\tau_j\,\mathrm{d}x + \int_{x_{j-1}}^{x_j}\psi\tau_j'\,\mathrm{d}x - \hat{\psi}(x)\tau_j(x)\Big|_{x_{j-1}}^{x_j} \\ & + \int_{x_{j-1}}^{x_j} Vz_j'\,\mathrm{d}x - \hat{V}(x)z_j(x)\Big|_{x_{j-1}}^{x_j} \\ & + k\int_{x_{j-1}}^{x_j} V\phi_j\,\mathrm{d}x - \int_{x_{j-1}}^{x_j} M\phi_j'\,\mathrm{d}x + \hat{M}(x)\phi_j(x)\Big|_{x_{j-1}}^{x_j}\Bigg\}\end{aligned} \tag{20}$$

where $\mathbf{v}|_K = (q_j,\tau_j,z_j,\phi_j) \in \mathcal{V}(K) = [H^1(K)]^4$ for each element $K = (x_{j-1},x_j) \in \mathcal{T}_h$, and equip the discontinuous test space

$$\mathcal{V}_h = \{\mathbf{v}\in[L_2(0,1)]^4,\ \mathbf{v}|_K \in \mathcal{V}(K),\ K\in\mathcal{T}_h\},$$

with the broken (element by element) inner product

$$(\mathbf{v},\delta\mathbf{v})_{\mathcal{V}_h} = \sum_{K\in\mathcal{T}_h}(\mathbf{v},\delta\mathbf{v})_{\mathcal{V}(K)} \tag{21}$$

Here the local inner product $(\cdot,\cdot)_{\mathcal{V}(K)}$ is chosen to correspond to that in Eq. (8).

The optimal test space $\mathcal{W}_h^{\mathrm{opt}} \in \mathcal{V}_h$ may now be defined as

$$\mathcal{W}_h = \{\mathbf{T}_h\mathbf{e}_1,\ldots,\mathbf{T}_h\mathbf{e}_n,\mathbf{T}_h\boldsymbol{\lambda}_h\} \tag{22}$$

where $\mathbf{T}_h : \mathcal{U}_n\times\boldsymbol{\Lambda}_h \to \mathcal{V}_h$ denotes the locally computable analogue of $\mathbf{T}:\mathcal{U}\to\mathcal{V}$ given by

$$(\mathbf{T}_h(\mathbf{u}_n,\boldsymbol{\lambda}_h),\delta\mathbf{v})_{\mathcal{V}_h} = \mathcal{B}_h(\mathbf{u}_n,\boldsymbol{\lambda}_h;\delta\mathbf{v}),\quad \forall\delta\mathbf{v}\in\mathcal{V}_h \tag{23}$$

Finally, the symmetrized variational problem to be solved is

$$\text{Find } \mathbf{u}_n\in\mathcal{U}_n,\ \boldsymbol{\lambda}_h\in\boldsymbol{\Lambda}_h \text{ s.t. } \mathcal{B}_h(\mathbf{u}_n,\boldsymbol{\lambda}_h;\mathbf{v}) = \mathcal{L}_h(\mathbf{v})\quad \forall\mathbf{v}\in\mathcal{W}_h \tag{24}$$

where $\mathcal{L}_h(\mathbf{v}) = Fz_N(1)$. Notice that the introduction of the interface variables $\boldsymbol{\lambda}_h$ enables the element-wise computation of the optimal broken test space $\mathcal{W}_h$, but they vanish from the picture on the continuous, one-element level because

$$\mathcal{B}_h(\mathbf{u}_n,\boldsymbol{\lambda}_h;\mathbf{v}) = \mathcal{B}(\mathbf{u}_n,\mathbf{v})\quad \&\quad \|\mathbf{v}\|_{\mathcal{V}_h} = \|\mathbf{v}\|_{\mathcal{V}}$$

for all globally continuous test functions $\mathbf{v}\in\mathcal{V}$. More precisely, we have the following (cf. [7])

Lemma 2.1 (Localization principle)**.** *The globally optimal test space $\mathcal{V}_n^{opt}$ defined by* (16) *is a subspace of the broken space $\mathcal{W}_h^{opt}$. Consequently, the subspace solutions $\mathbf{u}_n\in\mathcal{U}_n$ of Eqs.* (17) *and* (24) *coincide.*

Proof. Let us consider the component $z \in H^1(0,1)$ of the globally optimal test function $\mathbf{v} \in \mathcal{V}$. It is determined in terms of $V \in L_2(0,1)$ and $\hat{V}(0) \in \mathbb{R}$ through the equation

$$\int_0^1 (z'\delta z' + z\delta z)\,\mathrm{d}x = \int_0^1 V\delta z' + \hat{V}(0)\delta z(0) \quad \forall \delta z \in H^1(0,1)$$

If V is a smooth (trial) function within each element $K = (x_{j-1}, x_j)$, this variational problem corresponds to the interface problem

$$\begin{aligned} -z'' + z &= -V', && \text{in } (x_{j-1}, x_j),\ j = 1, \dots, N \\ [z' - V]_j &= 0, && j = 1, \dots, N-1 \\ z'(1) &= V(1) \\ -z'(0) &= \hat{V}(0) - V(0) \end{aligned}$$

where $[v]_j = v(x_j^+) - v(x_j^-)$ denotes the jump of v at x_j. Multiplying the differential equations by the corresponding local test functions $\delta z_j \in H^1(x_{j-1}, x_j)$, $j = 1, \dots, N$, integrating over each element, and then summing up the results gives

$$\sum_{j=1}^N \left\{ \int_{x_{j-1}}^{x_j} [-(z' - V)'\delta z_j + z\delta z_j]\,\mathrm{d}x \right\} = 0$$

Integrating the first term by parts, using the continuity of $z' - V$ at the nodes, and boundary conditions for z' at $x = 0, 1$, we obtain

$$\sum_{j=1}^N \left\{ \int_{x_{j-1}}^{x_j} (z'\delta z_j' + z\delta z_j)\,\mathrm{d}x \right\} = \sum_{j=1}^N \left\{ \int_{x_{j-1}}^{x_j} V\delta z_j' \right\} + \hat{V}(0)\delta v_1(0) + \sum_{j=2}^N (z' - V)(x_j)[\![\delta z]\!]_j$$

where $[\![\delta z]\!]_j = (\delta z_{j+1} - \delta z_j)(x_j)$. Since the local test functions δz_j are arbitrary, this shows that z can be represented as a linear combination of the locally optimal test functions corresponding to $V, \hat{V}(0)$ and the interface fluxes $\hat{\mathbf{V}} = ((z' - V)(x_1), \dots, (z' - V)(x_N))$. The corresponding result for the other components in $\mathbf{v}$ is obtained by similar reasoning. We leave the details for the reader. □

Lemma 2.1 implies that the best-approximation property (18) carries over to trial spaces associated to arbitrary partitions of the interval, i.e. we have the following result.

Theorem 2.2. *Let $\mathbf{u} = (V, M, w, \psi)$ denote the solution of the Timoshenko beam problem and $\mathbf{u}_n = (V_n, M_n, w_n, \psi_n)$ its approximation by the DPG method* (24) *with the optimal test space* (22) *corresponding to a chosen trial space associated to a partitioning* (19)*. Then $\mathbf{u}_n$ is the best approximation of $\mathbf{u}$ in the L_2-norm for all unknowns up to a positive constant independent of the thickness parameter t.*

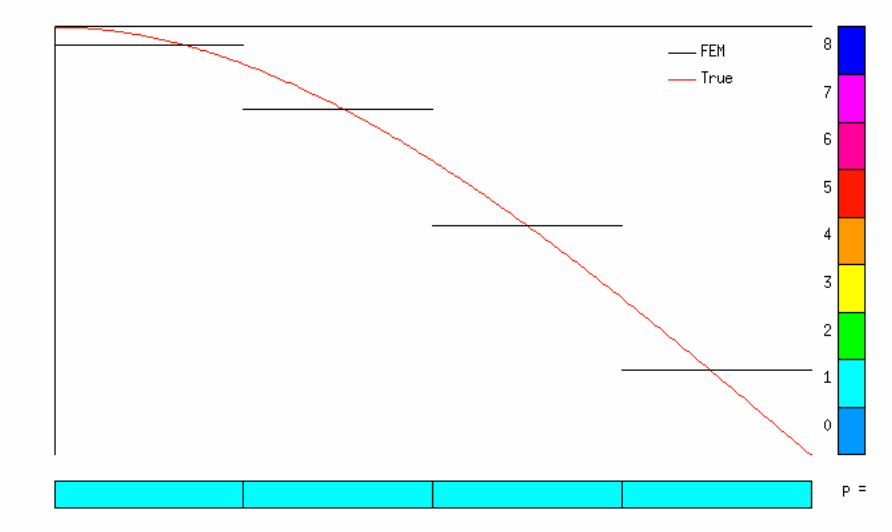

Figure 1: Transverse deflection $w = w(x)$ in the beam problem at $t/\gamma = 0$. DPG method with optimal test functions corresponding to four piecewise constant elements (black) and the exact solution (red).

Numerical experiments

To demonstrate the robustness of our method, we show here some results on the approximation of the asymptotic Euler-Bernoulli solution at $t/\gamma = 0$ with piecewise constant and piecewise linear elements. As is well known, strict enforcement of the classical Kirchhoff-Love constraint $\psi = w'$ by piecewise constant or piecewise linear finite elements leads to a trivial subspace without any approximation capabilities. Our results show that this is not a problem in the relaxed variational framework of the DPG method with optimal test functions.

We solved the problem numerically by approximating each of the field variables with piecewise polynomials of equal order associated to uniform subdivisions of the interval $(0, 1)$. The optimal test functions were resolved in an enriched finite element space obtained by increasing the polynomial degree of the local trial spaces in (23) by one.

Figures 1 and 2 show the approximative solutions with four piecewise constant and piecewise linear L_2-conforming elements[1], whereas the corresponding solutions with eight elements are shown in Figures 3 and 4.

Finally, Figure 5 shows the true error of the transverse deflection as measured in the L_2-norm for $t = 0.1$, $\gamma = 5/6$ and $t/\gamma = 0$. The convergence curves do not show any variation with respect to the thickness in accordance with the best approximation property predicted by Theorem 2.2.

[1]In all our figures the color-encoding represents the order of the corresponding H^1-conforming element which is one degree higher.

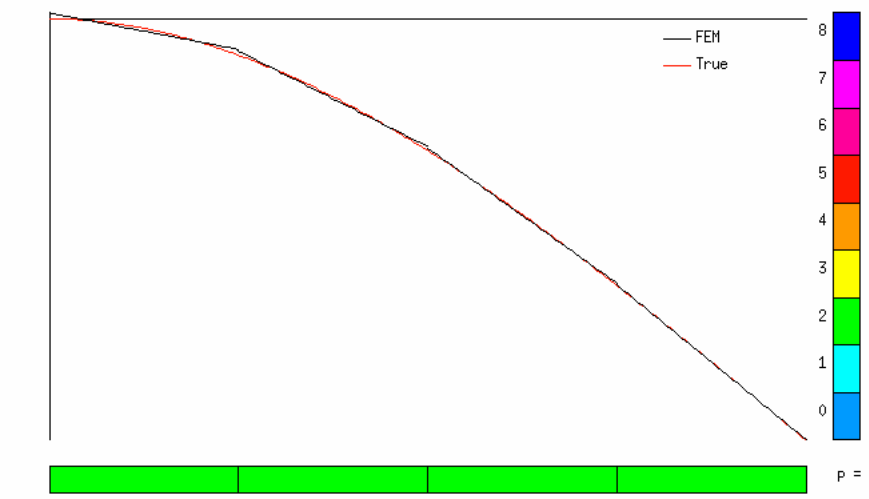

Figure 2: Transverse deflection $w = w(x)$ in the beam problem at $t/\gamma = 0$. DPG method with optimal test functions corresponding to four piecewise linear elements (black) and the exact solution (red).

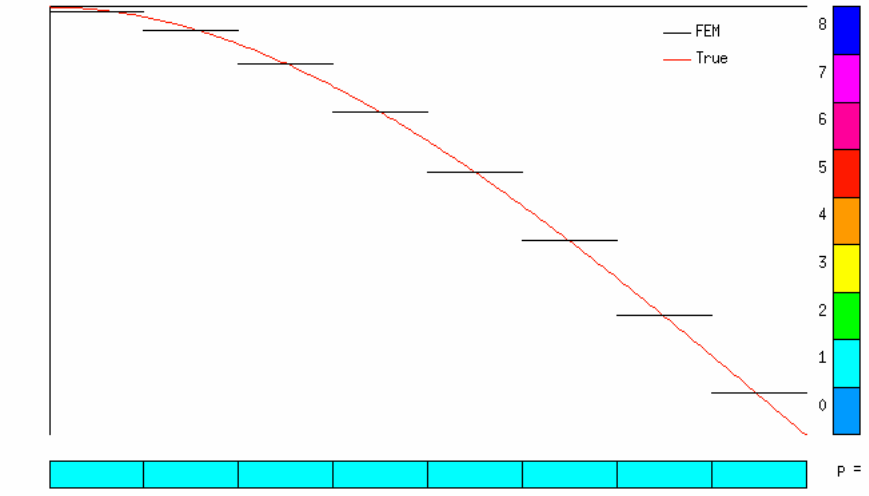

Figure 3: Transverse deflection $w = w(x)$ in the beam problem at $t/\gamma = 0$. DPG method with optimal test functions corresponding to eight piecewise constant elements (black) and the exact solution (red).

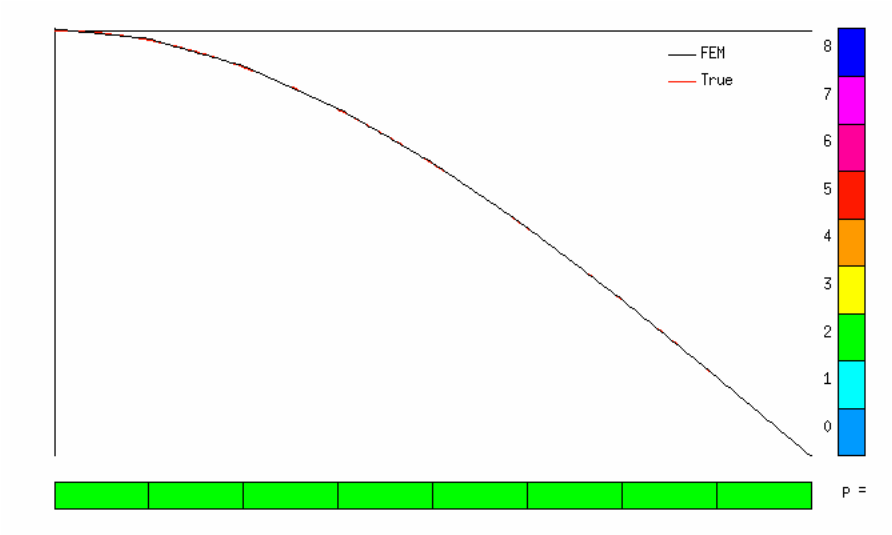

Figure 4: Transverse deflection $w = w(x)$ in the beam problem at $t/\gamma = 0$. DPG method with optimal test functions corresponding to eight piecewise linear elements (black) and the exact solution (red).

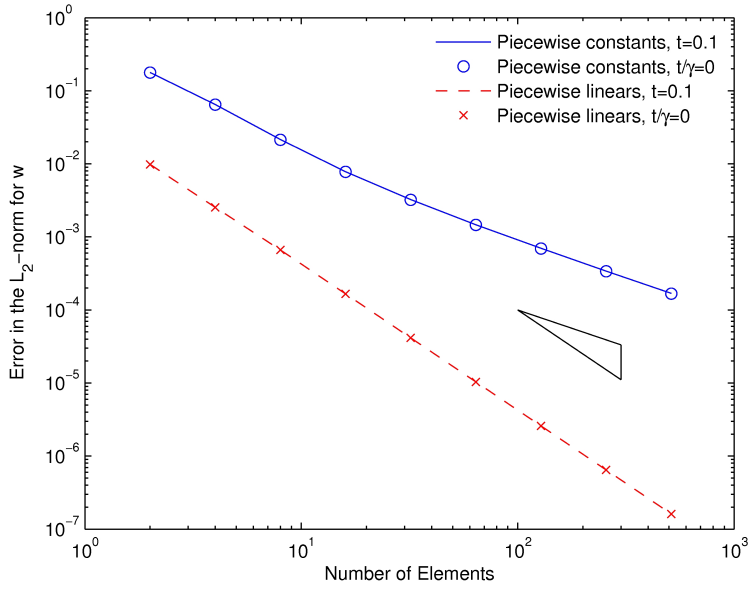

Figure 5: Convergence history in the beam problem for piecewise constant and linear elements.

3 Basic edge effect in shell deformations

We study here as a model problem axially symmetric deformations of a shallow spherical shell with radius R and thickness d, $d << R$. If x, y denote the (approximate, dimensionless) principal curvature coordinates on the shell mid-surface and there is no displacement in the y-direction, the kinematics of the shell can be described in terms of the single tangential displacement u, the transverse deflection w and the single rotation of the normal ψ:

$$u = u(x), \quad w = w(x), \quad \psi = \psi(x)$$

If the material is assumed homogenous and isotropic with Young's modulus E and Poisson ratio $\nu = 0$, the following scaled stresses may be introduced (see e.g. [9]):

$$\begin{aligned} T_x &= u' + w, & T_y &= w \\ V_x &= \gamma(w' - \psi), & M_x &= \frac{t^2}{12}\psi' \end{aligned} \tag{25}$$

Here we have taken R as the length unit, EdR as the force unit, and denoted the dimensionless shell thickness by $t = d/R$ while the shear correction factor γ has the same meaning as in the Timoshenko beam model. Because of the geometric curvature, the shear and bending reactions V_x and M_x are now coupled with the two membrane reactions T_x and T_y through the laws of static equilibrium:

$$\begin{aligned} -T_x' &= 0 \\ T_x + T_y - V_x' &= 0 \\ -M_x' - V_x &= 0 \end{aligned} \tag{26}$$

If we assume that the constant membrane stress T_x vanishes and rescale the shear force and bending moment as

$$V_x \hookrightarrow t^2 V, \quad M_x \hookrightarrow t^2 k^{-1} M, \quad k = 12$$

we arrive at the simplified shell equations

$$\begin{aligned} t^2 V &= \gamma(w' - \psi), & M &= \psi' \\ w - t^2 V' &= 0, & -M - kV &= 0 \end{aligned} \tag{27}$$

resembling the beam equations (4). Nevertheless, here the problem cannot be solved by direct elimination of the unknowns because of the coupling of w and V in the first equilibrium equation. The equations (27) constitute anyway a system of ordinary differential equations with constant coefficients so that the solutions $\mathbf{u} = (V, M, w, \psi)$ take the form

$$\mathbf{u}(x) = e^{\lambda x}\mathbf{U}$$

where the possible values of λ are found as the roots of the characteristic polynomial

$$p(\lambda) = t^2\gamma\lambda^4 - t^2\lambda^2 + 12\gamma$$

Therefore the solutions of (27) take the boundary-layer form (cf. [9, 10])

$$\mathbf{u} = e^{ax}(\mathbf{A}(t)\cos(bx) + \mathbf{B}(t)\sin(bx)), \quad a \approx b \approx \pm 3^{1/4}/\sqrt{t} \tag{28}$$

corresponding to the so called basic, or simple edge effect in shell deformations.

Variational form

We consider as a model problem the approximation of a boundary layer mode $\mathbf{u} = (V, M, w, \psi)$ of Eq. (28) that decays exponentially from $x = 0$ with the length scale $L = \mathcal{O}(\sqrt{t})$ and is normalized such that $M(0) = 1$. The corresponding values of $V(0)$ and $w(1) \approx \psi(1) \approx 0$ are taken as the remaining essential boundary conditions. The continuous, one-element bilinear form is then

$$\begin{aligned}\mathcal{B}(\mathbf{u}, \mathbf{v}) = t^2 \int_0^1 Vq \,\mathrm{d}x + \gamma \int_0^1 wq' \,\mathrm{d}x + \gamma \hat{w}(0)q(0) + \gamma \int_0^1 \psi q \,\mathrm{d}x \\ + \int_0^1 M\tau \,\mathrm{d}x + \int_0^1 \psi\tau' \,\mathrm{d}x + \hat{\psi}(0)\tau(0) \\ + \int_0^1 wz \,\mathrm{d}x + t^2 \int_0^1 Vz' \,\mathrm{d}x - \widehat{t^2V}(1)z(1) \\ + k \int_0^1 V\phi \,\mathrm{d}x - \int_0^1 M\phi' \,\mathrm{d}x + \hat{M}(1)\phi(1)\end{aligned} \tag{29}$$

where the variational setting for $\mathbf{u} = (V, M, \psi, w) \times (\hat{w}(0), \hat{\psi}(0), \widehat{t^2V}(1), \hat{M}(1)) \in \mathcal{U}$ and $\mathbf{v} = (V, M, z, \phi) \in \mathcal{V}$ remain the same as in the beam problem (the prescribed boundary terms are incorporated into the right-hand side $\mathcal{L}$).

Because of the non-trivial parametric dependence of the problem, the use of standard test space norm (8) does not lead to a generalized energy norm $|||\cdot|||$ equivalent to the regular L_2-norm uniformly in t as in the beam problem. However, if we instead equip the test space with a dual norm

$$\|\mathbf{v}\|_{\mathcal{V}} = \sup_{\mathbf{v} \in \mathcal{V}} \frac{\mathcal{B}(\mathbf{u}, \mathbf{v})}{\|\mathbf{u}\|_{\mathcal{U}}} \tag{30}$$

corresponding to a chosen norm for the trial space, we will have $|||\cdot||| = \|\cdot\|_{\mathcal{U}}$. The Hilbert space norm corresponding to (30) to be used in computations may be derived by regrouping the terms in the bilinear form as

$$\begin{aligned}\mathcal{B}(\mathbf{u}, \mathbf{v}) = \int_0^1 V(t^2q + t^2z' + k\phi) \,\mathrm{d}x + \int_0^1 M(\tau - \phi') \,\mathrm{d}x \\ + \int_0^1 w(\gamma q' + z) \,\mathrm{d}x + \int_0^1 \psi(\gamma q + \tau') \,\mathrm{d}x \\ + \gamma\hat{w}(0)q(0) + \hat{\psi}(0)\tau(0) - \widehat{t^2V}(1)z(1) + \hat{M}(1)\phi(1)\end{aligned}$$

If $\|\cdot\|_{\mathcal{U}}$ is chosen as in (10), it is rather easy to see that the norm (30) squared becomes

$$\begin{aligned}\|\mathbf{v}\|_{\mathcal{V}}^2 = \left\|t^2(q + z') + k\phi\right\|^2 + \|\tau - \phi'\|^2 + \|\gamma q' + z\|^2 + \|\gamma q + \tau'\|^2 \\ + |\gamma q(0)|^2 + |\tau(0)|^2 + |z(1)|^2 + |\phi(1)|^2\end{aligned} \tag{31}$$

on the continuous, one-element level. Obviously, the localization principle (Lemma 2.1)

becomes violated if this norm is used, but it can be restored by redefining (31) e.g. as

$$\begin{aligned}\|\mathbf{v}\|_{\mathcal{V}}^2 = &\left\|t^2(q+z')+k\phi\right\|^2 + \|\tau-\phi'\|^2 + \|\gamma q+\tau'\|^2 + \|\gamma q'+z\|^2 \\ &+ \|\gamma q\|^2 + \|\tau\|^2 + \|z\|^2 + \|\phi\|^2\end{aligned} \tag{32}$$

Because the leading terms involving the derivatives remain the same, it is very likely that the modification will not affect the robustness of method. Our numerical experiments confirm this.

A posteriori error estimation. Adaptivity

In order to resolve the boundary layer in our model problem, the finite element mesh must be refined towards $x = 0$. As shown in [7], this can be achieved in an automatic manner by utilizing the discontinuous variational framework.

The generalized energy norm of the error $\mathbf{e} = \mathbf{u} - \mathbf{u}_n$ is defined as $|\!|\!|\mathbf{e}|\!|\!| = \|\mathbf{Te}\|_{\mathcal{V}}$ where

$$(\mathbf{Te}, \delta\mathbf{v})_{\mathcal{V}} = \mathcal{B}(\mathbf{e}, \delta\mathbf{v}) = \mathcal{L}(\delta\mathbf{v}) - \mathcal{B}(\mathbf{u}_n, \delta\mathbf{v}) \quad \forall \delta\mathbf{v} \in \mathcal{V}$$

By the localization principle, the error representation function $\mathbf{Te}$ may be determined elementwise from

$$(\mathbf{T}_h\mathbf{e}, \delta\mathbf{v})_{\mathcal{V}_h} = \mathcal{L}_h(\delta\mathbf{v}) - \mathcal{B}_h(\mathbf{u}_n, \boldsymbol{\lambda}_h; \delta\mathbf{v}) \quad \forall \delta\mathbf{v} \in \mathcal{V}_h$$

so that the energy norm of the error is obtained by summing over the elements

$$|\!|\!|\mathbf{e}|\!|\!|^2 = \sum_{K\in\mathcal{T}_h} \|\mathbf{T}_h\mathbf{e}\|_{\mathcal{V}(K)}^2 \tag{33}$$

The individual element error contributions $\eta_K = \|\mathbf{T}_h\mathbf{e}\|_{\mathcal{V}(K)}^2$ can be used directly to guide adaptive mesh refinements.

Numerical experiments

In our numerical experiments with the shell problem, the field variables are approximated by piecewise polynomials of equal but variable order associated to arbitrary subdivisions of the interval $(0, 1)$. Because of the more challenging nature of the problem, we used an increment of three in the polynomial order when computing the approximate optimal test functions. We have used both norms (32) and (8), i.e. optimal and standard, for the test space.

Proceeding from the initial mesh consisting of four piecewise linear elements shown in Figures 6 and 7 for the optimal and standard test space norm, respectively, we construct adaptively refined meshes as follows. An element K is tagged for refinement if the corresponding error indicator shows a value larger than 25% of the maximum value over all elements, i.e. $\eta_K \geq 0.25 \cdot \max_{K\in\mathcal{T}_h} \eta_K$. Concerning the type of refinement, the elements are broken in space until the boundary layer length scale $L = 3^{-1/4}\sqrt{t}$ is reached after which their order is being raised.

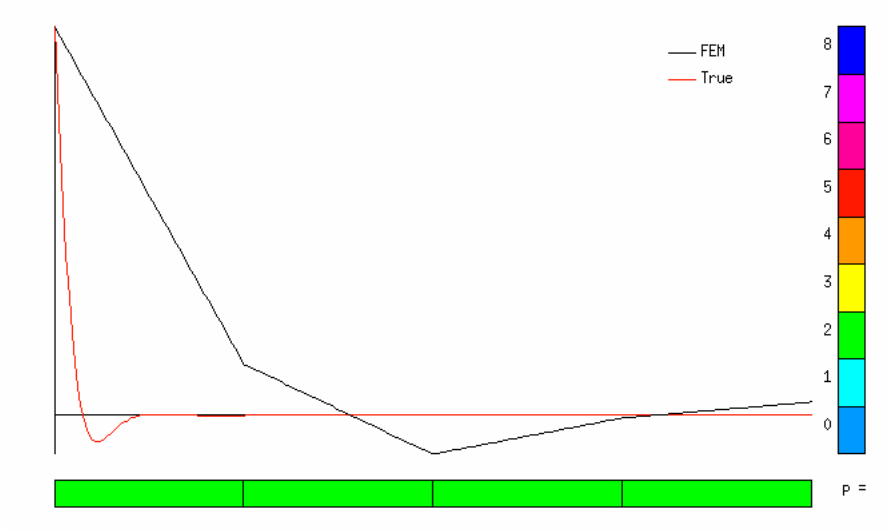

Figure 6: Bending moment $M = M(x)$ in the shell problem at $t = 1/1000$. Initial mesh with the optimal test space norm.

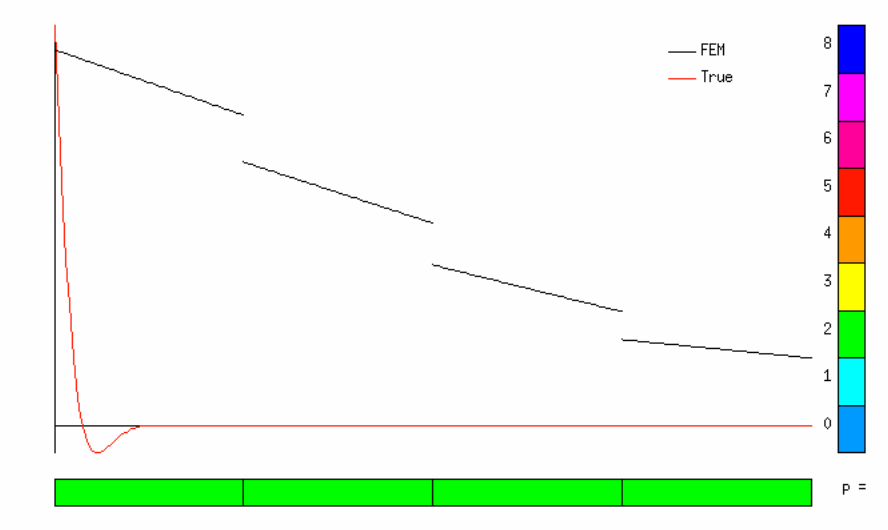

Figure 7: Bending moment $M = M(x)$ in the shell problem at $t = 1/1000$. Initial mesh with standard test space norm.

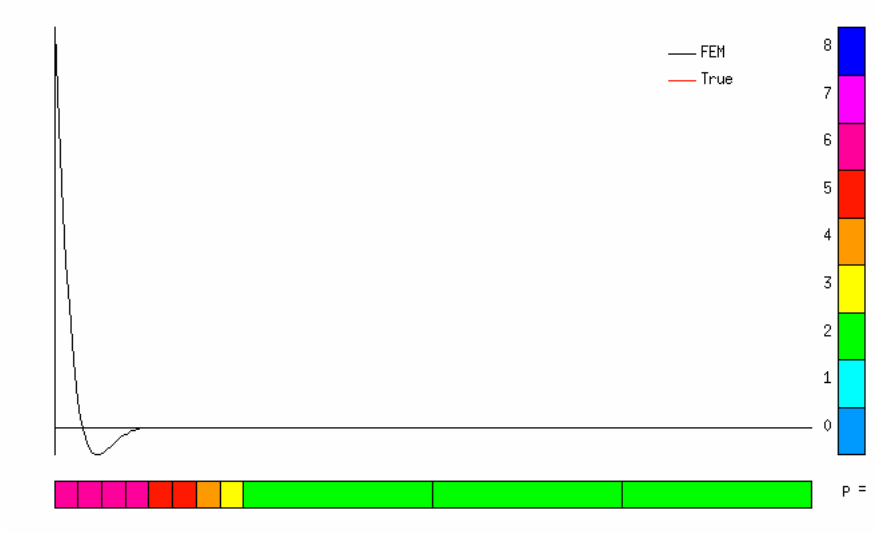

Figure 8: Bending moment $M = M(x)$ in the shell problem at $t = 1/1000$. DPG method with the optimal test space norm corresponding to an automatically generated *hp*-mesh with 236 D.O.F. (black) overlaps the true solution (red)

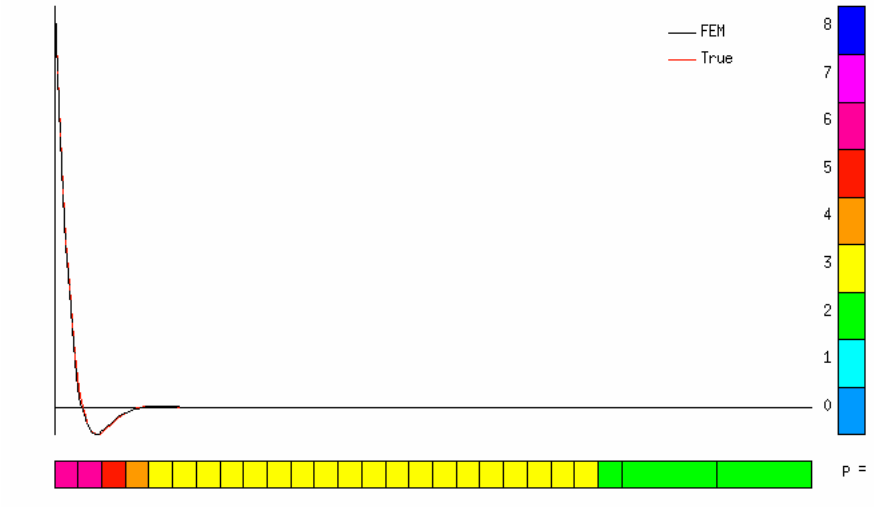

Figure 9: Bending moment $M = M(x)$ in the shell problem at $t = 1/1000$. DPG method with the standard test space norm corresponding to an automatically generated *hp*-mesh with 444 D.O.F. (black) and the true solution (red).

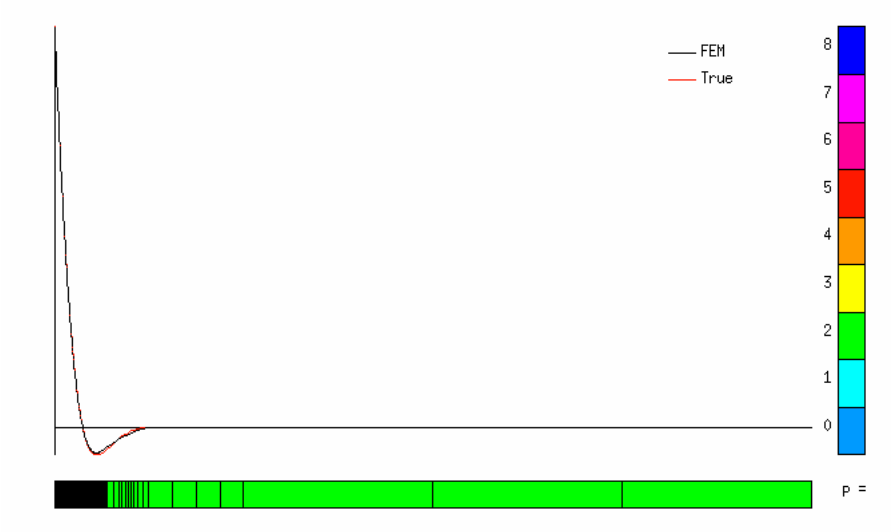

Figure 10: Bending moment $M = M(x)$ in the shell problem at $t = 1/1000$. DPG method with optimal test functions corresponding to an automatically generated h-mesh with 1360 D.O.F. (black) and the true solution (red).

Figures 8 and 9 show the final hp-mesh corresponding to the optimal and standard test space norms. The superiority of the optimal test space norm over the standard one is rather evident as the quality of the solution is better with less degrees of freedom.

We considered also pure h-refinements as an alternative mesh optimization strategy. The optimized mesh after ten refinement sweeps is shown in Figure 10 for piecewise linear elements and in Figure 11 for piecewise quadratic elements. Here we have relied on the optimal test norm as the standard one does not work so well with low-order polynomials. Comparison with Figure 8 shows clearly how a good hp-refinement strategy delivers an extremely accurate solution by distributing the degrees of freedom in a more economic way than traditional h-refinements.

4 Concluding remarks

We have taken the first steps in the study of discontinuous Petrov-Galerkin methods with optimal test functions in the context of solid mechanics. In particular, we have introduced a robust, locking-free formulation for beam problems. A nice feature of the proposed formulation is that it can be used to model moderately thick beams with non-vanishing transverse shear deformation as well as the asymptotic bending behaviour of thin beams described by the Euler-Bernoulli model.

We have also demonstrated the potential of the DPG variational framework for automatic hp-adaptivity which helps e.g. to resolve boundary layers in shell deformations. With a proper choice of the norm for the test space, the adaptive process leads to refinements in

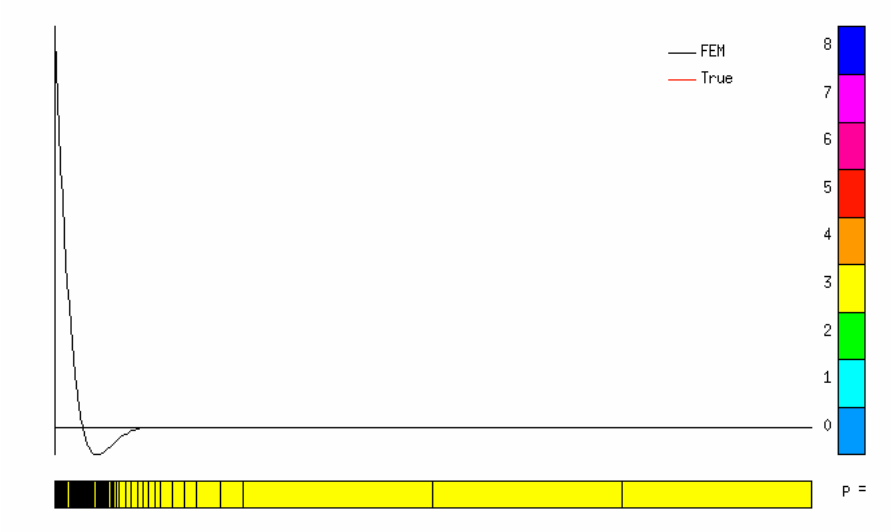

Figure 11: Bending moment $M = M(x)$ in the shell problem at $t = 1/1000$. DPG method with optimal test functions corresponding to an automatically generated h-mesh with 884 D.O.F. (black) overlaps the true solution (red).

regions where maximum stresses occur and can be started with an initial mesh consisting of few low-order elements only .

Based on our numerical and theoretical experience, we are hopeful regarding the extension of these techniques to two-dimensional plate and shell problems as well as to more general problems in Cosserat continuum.

References

[1] L. Demkowicz, J. Gopalakrishnan, A class of discontinuous Petrov-Galerkin methods. Part I: The transport equation, ICES Report 09-12 (2009) 1–29.

[2] L. Demkowicz, J. Gopalakrishnan, A class of discontinuous Petrov-Galerkin methods. Part II: Optimal test functions, ICES Report 09-16 (2009) 1–34.

[3] J. Barrett, K. Morton, Approximate symmetrization and Petrov-Galerkin methods for diffusion-convection problems, Comput. Methods Appl. Mech. Engrg. 45 (1984) 97–122.

[4] L. Demkowicz, J. T. Oden, An adaptive characteristic Petrov-Galerkin finite element method for convection-dominated linear and nonlinear parabolic problems in one space variable, J. Comput. Phys. 67 (1986) 188–213.

[5] L. Demkowicz, J. T. Oden, An adaptive characteristic Petrov-Galerkin finite element method for convection-dominated linear and nonlinear parabolic problems in two space variables, Comput. Methods Appl. Mech. Engrg. 55 (1986) 63–87.

[6] C. L. Bottasso, S. Micheletti, R. Sacco, The discontinuous Petrov-Galerkin method for elliptic problems, Comput. Methods Appl. Mech. Engrg. 191 (2002) 3391–3409.

[7] L. Demkowicz, J. Gopalakrishnan, A. H. Niemi, A class of discontinuous Petrov-Galerkin methods. Part III: Adaptivity, ICES Report 10-01 (2010) 1–37.

[8] J. Pitkäranta, Mathematical and historical reflections on the lowest-order finite element models for thin structures, Comput. Struct. (81) (2003) 895–909.

[9] J. Pitkäranta, A.-M. Matache, C. Schwab, Fourier mode analysis of layers in shallow shell deformations, Comput. Methods Appl. Mech. Engrg. 190 (2001) 2943–2975.

[10] A. H. Niemi, Approximation of shell layers using bilinear elements on anisotropically refined rectangular meshes, Comput. Methods Appl. Mech. Engrg. 197 (2008) 3964–3975.

[11] A. H. Niemi, A bilinear shell element based on a refined shallow shell model, Int. J. Numer. Meth. Engng 81 (2010) 485–512.

[12] F. Béchet, E. Sanchez-Palencia, O. Millet, Singularities in shell theory: Anisotropic error estimates and numerical simulations, Comput. Methods Appl. Mech. Engrg. 199 (2010) 13261341.

[13] D. N. Arnold, R. S. Falk, Asymptotic analysis of the boundary layer for the reissner-mindlin plate model, Siam J. Math. Anal. 27 (1996) 486–514.

[14] L. Beirão da Veiga, J. Niiranen, R. Stenberg, A family of c^0 finite elements for Kirchhoff plates I: error analysis, Siam J. Numer. Anal. 45 (2007) 20472071.

[15] A. F. Loula, T. J. Hughes, L. P. Franca, Petrov-Galerkin formulations of the Timoshenko beam problem, Comput. Methods Appl. Mech. Engrg. 63 (1987) 115–132.

[16] A. F. Loula, T. J. Hughes, L. P. Franca, I. Miranda, Mixed Petrov-Galerkin methods of the Timoshenko beam problem, Comput. Methods Appl. Mech. Engrg. 63 (1987) 133–154.

[17] A. F. D. Loula, L. P. Franca, T. J. R. Hughes, I. Miranda, Stability, convergence and accuracy of new finite element method for the circular arch problem, Comput. Methods Appl. Mech. Engrg. 63 (1987) 281–303.

[18] L. P. Franca, T. J. R. Hughes, A. F. D. Loula, I. Miranda, A new family of stable elements for nearly incompressible elasticity based on a mixed petrov-galerkin finite element formulation, Numer. Math. 53 (1988) 123–141.

[19] J. T. Oden, L. F. Demkowicz, Applied functional analysis, CRC Press, United States of America, 2009.